



**HAL**  
open science

## Effect of ion irradiation on aluminium hydroxide in an Al-Mg-Si alloy

S. L'Haridon-Quaireau, K. Colas-Leroux, B. Kapusta, B. Verhaeghe, V. Cloute-Cazalaa, S Delpech, G. Gutierrez, M. Loyer-Prost, D. Gosset

► **To cite this version:**

S. L'Haridon-Quaireau, K. Colas-Leroux, B. Kapusta, B. Verhaeghe, V. Cloute-Cazalaa, et al.. Effect of ion irradiation on aluminium hydroxide in an Al-Mg-Si alloy. 19th Meeting of the International Group on Research Reactors (RRFM/IGORR - 2019), Mar 2019, Kazan, Jordan. cea-02394064

**HAL Id: cea-02394064**

**<https://cea.hal.science/cea-02394064>**

Submitted on 24 Feb 2020

**HAL** is a multi-disciplinary open access archive for the deposit and dissemination of scientific research documents, whether they are published or not. The documents may come from teaching and research institutions in France or abroad, or from public or private research centers.

L'archive ouverte pluridisciplinaire **HAL**, est destinée au dépôt et à la diffusion de documents scientifiques de niveau recherche, publiés ou non, émanant des établissements d'enseignement et de recherche français ou étrangers, des laboratoires publics ou privés.

# EFFECT OF ION IRRADIATION ON ALUMINIUM HYDROXIDE IN AN AL-MG-SI ALLOY

S. L'HARIDON-QUAIREAU, K. COLAS, B. KAPUSTA, B. VERHAEGHE, V. CLOUTE-CAZALAA

*DEN-Service d'Etude des Matériaux Irradiés, CEA, Université Paris-Sud  
F-91191, Gif-sur-Yvette - France*

S. DELPECH

*IPNO, Paris-Sud University  
Paris - France*

G. GUTIERREZ, M. LOYER-PROST

*DEN-Service de Recherche de Métallurgie Physique, CEA, Université Paris-Sud  
F-91191, Gif-sur-Yvette - France*

D. GOSSET

*DEN-Service de Recherche de Métallurgies Appliquées, CEA, Université Paris-Sud  
F-91191, Gif-sur-Yvette - France*

## ABSTRACT

In the core of a nuclear reactor, irradiation defects created by the fast neutron flux can have a detrimental effect on the corrosion of aluminium alloys. In order to better understand the effect of irradiation on aluminium corrosion, a hydroxide obtained by corrosion of an Al-Mg-Si alloy is irradiated with Al ions. The damage created is 2.5 dpa (displacement per atom) on average in the aluminium hydroxide (Stopping and Range of Ions in Matter (SRIM) calculation). The ion irradiation seems to cause an amorphization of the hydroxide. Voids and nano-crystallites can also be observed. After re-corrosion of the irradiated hydroxide, an increase of the thickness of the oxide layer can be observed compared to the non-irradiated oxide.

## 1. Introduction

Aluminium alloys are used in many fields, in particular for nuclear research reactors (NRRs). Due to a low activation, neutron transparency and good mechanical properties, aluminium alloys are used in nuclear cores of NRRs for the core components or for the fuel cladding [1]. However, these aluminium alloys are corroded in the nuclear core: an aluminium hydroxide covers their surface. The thermal conduction of this hydroxide is low (~2 W/m/K [2]): the hydroxide degrades heat exchanges between the components and the water of the primary circuit. It could therefore lead to an overheating of the components. As a result, the study of aluminium alloys corrosion is important for the safe and efficient operation of NRRs.

In this context, some authors studied the corrosion of aluminium alloys in nuclear research reactors or in corrosion loops.

Pawel et al. [3]–[5] and Griess et al. [6]–[9] studied the corrosion of aluminium alloys in corrosion loops with conditions representative of NRRs. Their corrosion tests allowed creating a model. This model was used to estimate the hydroxide thickness on aluminium alloys used in NRRs. However, this model misestimated the hydroxide thickness: the thicknesses measured on aluminium alloys corroded in nuclear core were not close to the one predicted [10]. Indeed, during their corrosion tests, the irradiation was not taken into account and corrosion tests conducted in nuclear reactor by Kim et al. [10] revealed an effect of the damage in the aluminium hydroxide created by the neutron irradiation. As a result, the model of Pawel and Griess was reassessed by Kim to take into account the effect of the irradiation. However,

the impact of the irradiation damage on aluminium hydroxide is not well known. As a result, new studies about the effect of the irradiation on aluminium hydroxide are required. In this study, in order to analyse the effect of the irradiation on aluminium corrosion without dealing with radioactive samples, ion irradiation is used to simulate the irradiation damage.

## 2. Experiments

The samples are in AA6061-T6 aluminium alloy. This alloy is mainly composed by Al (balance), Fe (0.7%mass), Si (0.4-0.8 %mass), Cu (0.15-0.4%mass) and Mg (0.8-1.2%mass) [11]. Before corrosion test, the samples are polished down to a 1  $\mu\text{m}$  finish with diamond paste. In order to obtain an aluminium hydroxide film on the aluminium samples, corrosion experiment is performed in autoclave (V=5.5L, 316L steel, inside covered with Teflon) on aluminium alloy samples (10 x 10 x 1 mm). The samples are corroded at 70°C, for 7 days and in 2.8L of pure water. This corrosion test allows obtaining an aluminium hydroxide film on the samples surface. The thickness of this film is about 4  $\mu\text{m}$ . The crystal phase of this hydroxide is studied by low-incidence X-ray diffraction (XRD, diffractometer with Cu-K $\alpha$  radiation in asymmetric configuration, the incident angle of the X-ray beam is 2°) and  $\mu$ -Raman spectroscopy (P=100 mW and  $\lambda$ =532 nm).

After the corrosion test, the samples are irradiated with ions. The ions are Al ions with successive energies of 1.2 MeV and 5 MeV in order to have a nearly homogenous damage profile in the hydroxide layer. A SRIM calculation (using the Stopping and Range of Ions in Matter software) indicates the damage is at most 4.5 dpa (displacement per atom) and 2.5 dpa on average in the aluminium hydroxide. The Al ions implantation peaks are located at a depth of 1.4  $\mu\text{m}$  for the ions with an energy of 1.2 MeV and of 3.1  $\mu\text{m}$  with an energy of 5 MeV. For the SRIM calculation, the threshold displacement energies used are 20 eV and 50 eV for the aluminium and oxygen sublattice, respectively [12].

After the ion irradiation, some irradiated samples are corroded a second time in order to study the impact of ion irradiation on the corrosion kinetics. For this corrosion experiment, the conditions are 4 days, 70°C and 2.8 L of pure water.

Before and after the ion irradiation, the aluminium hydroxide is examined using Scattering Electron Microscopy (SEM), Transmission Electron Microscopy (TEM, with an acceleration voltage of 300 kV and a length camera of 865 mm), XRD analyses and  $\mu$ -Raman spectroscopy. In order to examine the cross section of the hydroxide using a SEM, some samples are embedded in conductive resin and polished down to a 1  $\mu\text{m}$  finish with diamond pastes. TEM samples of the corroded materials are prepared with conventional Focused Ion Beam (FIB) methods. A Pt deposit is added on the samples surface to protect the hydroxide during the manufacturing of the TEM samples.

## 3. Results

The effect of the ion irradiation on aluminium hydroxide is evaluated by examining the hydroxide layer before and after irradiation. The results of these examinations are presented in the following paragraphs.

Also in order to evaluate the impact of irradiation on hydroxide growth, the irradiated samples are re-corroded. The results of this corrosion test are described in the last part.

### 3.1 Aluminium hydroxide before irradiation

Before ion irradiation, the aluminium hydroxide film is composed of two layers: an inner and an outer layer, as seen in Fig 1.b. The outer layer, in contact with the aqueous media, is a crystalline hydroxide: micro-crystals of aluminium hydroxide are observed on the samples surface as seen in Fig 1.a. The  $\mu$ -Raman spectrum of this outer layer indicates it is composed of bayerite ( $\alpha$ -Al(OH)<sub>3</sub>, Fig 1.c, Raman peaks of bayerite : [13]).

Between the bayerite layer and the aluminium matrix, the inner layer is composed of a non-fully crystallised phase. The peaks of the  $\mu$ -Raman signal obtained on this inner layer can be

attributed to boehmite ( $\gamma\text{-AlOOH}$ , Fig 1.c, Raman peaks of boehmite : [13], [14]); however, the peaks are poorly defined. From this Raman spectrum, it can be concluded the inner layer is pseudo-boehmite (a nanocrystalline boehmite phase). This hydroxide is often found on surface of aluminium alloys during aqueous corrosion tests at all temperature [15].

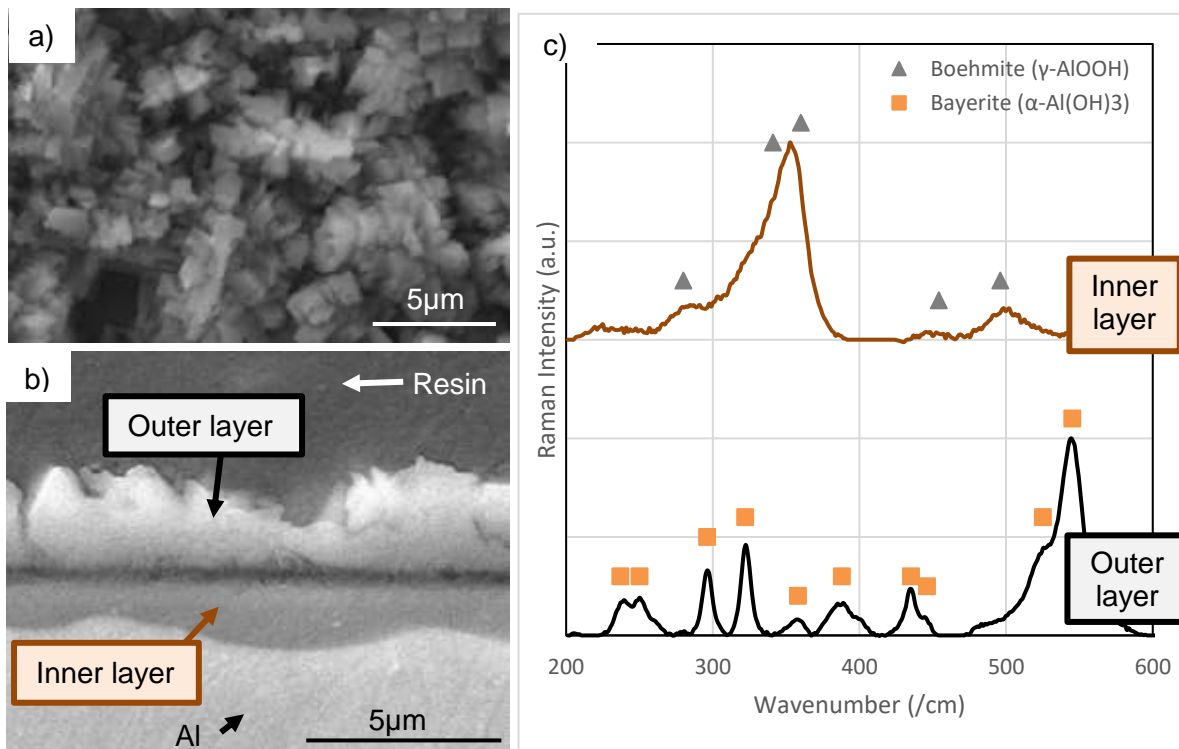


Fig 1. (a) Aluminium hydroxide crystals of the outer layer at the surface of the samples (top view, SEM, secondary electron mode), (b) cross section of the aluminium hydroxide found on the samples (SEM, secondary electron mode); (c)  $\mu$ -Raman spectra obtained on the inner and outer layers.

A low incidence X-ray diffraction on the corrosion products confirms the results of  $\mu$ -Raman analyses (Fig. 3): bayerite is the main crystalline phase formed during the corrosion experiments; traces of boehmite are also present. This composition of the hydroxide is common at 70°C, the temperature of the corrosion test, according to the literature [1], [15].

### 3.2 Irradiated aluminium hydroxide

The Fig. 2.a presents a cross section of the irradiated oxide observed by TEM. The irradiated oxide is between the Pt deposit and the aluminium matrix. After ion irradiation, the distinction between the two former layers (inner and outer layers) is difficult as seen in Fig. 2.a. The outer layer is amorphized: the former micro-crystals of bayerite could not be observed. In addition, voids are present in the irradiated oxide, in the two layers. A line of voids is observed in the middle of the former inner layer. This line corresponds to the peak of damage made by the Al ions in the inner layer (i.e. at 4.5 dpa).

Additionally, an electron diffraction observation is performed on the irradiated oxide (Fig. 2.b). The rings obtained from this electron diffraction indicate the presence of nano-crystallites. A dark field performed on the ring of 1.39 Å is presented in Fig 2.c: the nano-crystallites that have diffracted to form this ring are in white in the oxide matrix in black.

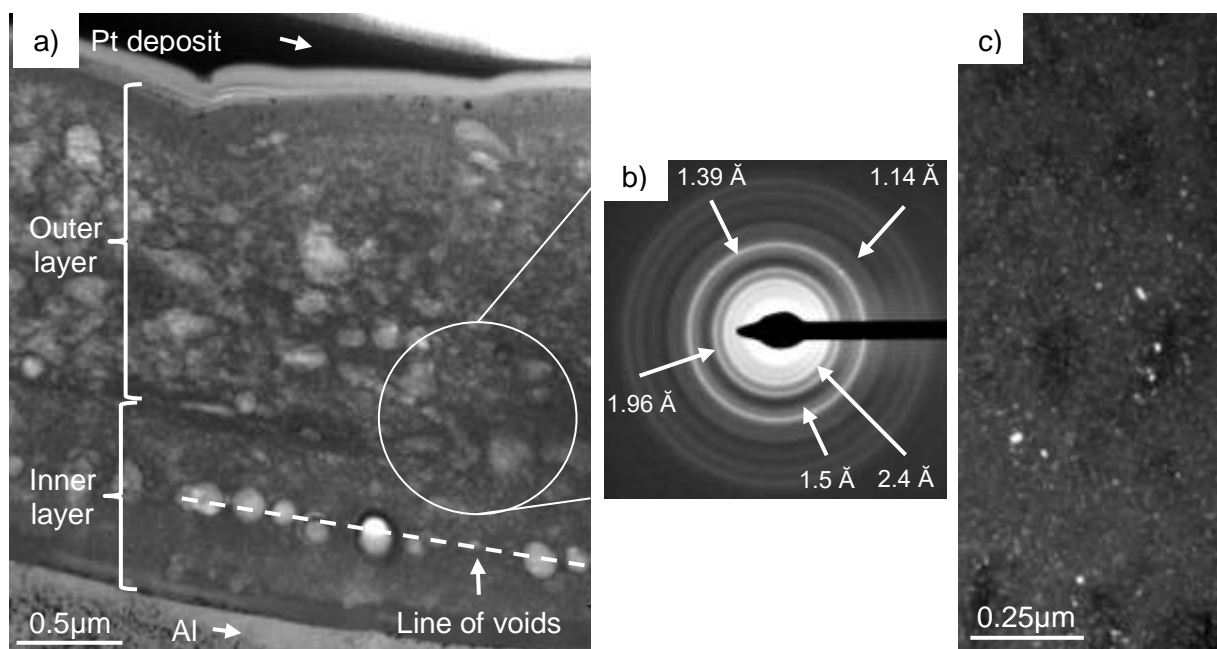


Fig 2. (a) Cross section of irradiated oxide (TEM), (b) electron diffraction pattern obtained from the irradiated oxide, attributed to  $\eta$ -Al<sub>2</sub>O<sub>3</sub>, and (c) Dark Field of the crystallites (in white) in the oxide (in black) that have diffracted to form the ring at 1.39Å.

The electron diffraction pattern on Fig 2.b can be attributed to a nanometric  $\eta$ -Al<sub>2</sub>O<sub>3</sub> phase: the d-spacing measured at 1.14Å, 1.39Å, 1.50Å, 1.96Å and 2.40Å are very close to those measured by Tilley for the nanometric  $\eta$ -Al<sub>2</sub>O<sub>3</sub> phase in bauxite [16].

In the literature [15], this oxide phase comes from the thermal decomposition of bayerite and pseudo-boehmite at 250-650°C. However, during the irradiation, the maximal temperature of the irradiated hydroxide is 20°C (a thermocouple is placed in contact with the oxide during the irradiation). As a result, the presence of  $\eta$ -Al<sub>2</sub>O<sub>3</sub> cannot be attributed to a temperature but could be due to the ion irradiation.

In addition, when the irradiation starts, the pressure of the vacuum in the accelerator increases from 10<sup>-8</sup> Pa to 10<sup>-7</sup> Pa: due to the ion beam, the former aluminium hydroxide could be decomposed into  $\eta$ -Al<sub>2</sub>O<sub>3</sub> by releasing water.

Unfortunately, the presence of  $\eta$ -Al<sub>2</sub>O<sub>3</sub> could not be confirmed by a Raman analysis: after irradiation, the laser light is strongly diffused by the oxide, which makes impossible to realize a measurement of sufficient quality of the oxide. This type of problem is common with this aluminium oxide [17].

Additionally, the  $\eta$ -Al<sub>2</sub>O<sub>3</sub> phase could not be observed in the X-ray diffraction diagram of the irradiated hydroxide (Fig 3): it can be due to the small size of the crystallites (>10nm, Fig 2.c) and the insufficient resolution of the diffractometer. In addition, the main peaks of  $\eta$ -Al<sub>2</sub>O<sub>3</sub> at 37.80° [16] is very close to the peaks of aluminium at 38.4° [18], a distinction between the two phases is impossible. However, the peaks of bayerite are still present in this spectrum but a decrease in intensity of the peaks is observed. This result can be attributed to an important amorphization of the bayerite.

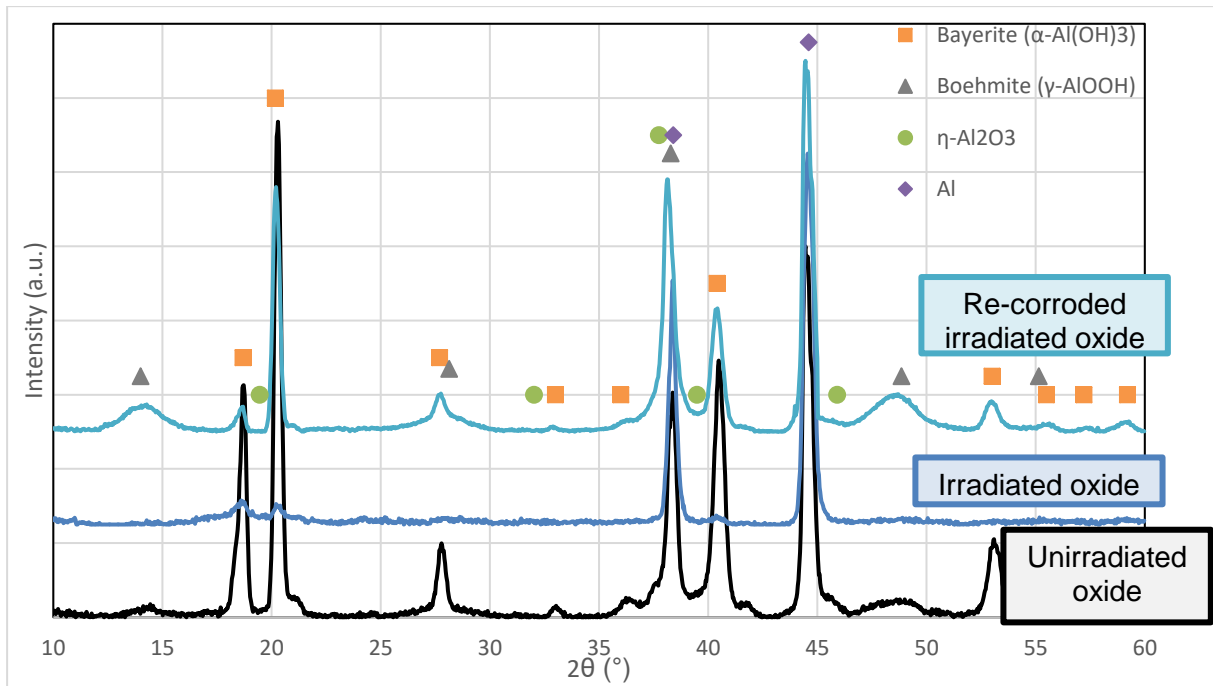


Fig 3. X-rays diffraction spectra of the aluminium hydroxide in different conditions (before and after irradiation and after re-corrosion of the irradiated oxide)

### 3.3 Effect of ion irradiation on corrosion kinetics

After ion irradiation, the samples are re-corroded in order to evaluate the effect of the irradiation on hydroxide growth.

After the re-corrosion of the irradiated oxide, two layers of aluminium hydroxide are present at the samples surface as seen on the picture of re-corroded irradiated oxide in Fig. 4. The inner layer, near the aluminium matrix, is pseudo-boehmite and the outer layer is bayerite ( $\mu$ -Raman analyses, confirmed by XRD analysis on Fig 3). The thickness of these two layers is measured on a cross section of the hydroxide embedded in resin and observed with SEM (Fig 4).

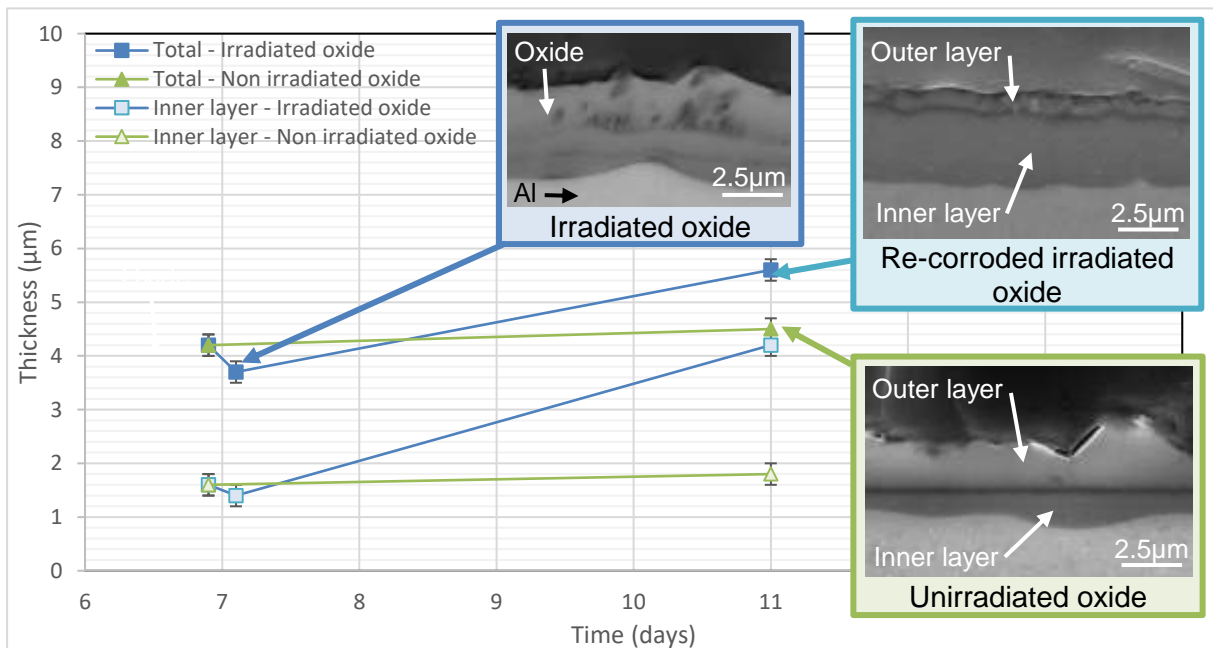


Fig 4. Evolution of the thickness of irradiated and unirradiated hydroxides and micrographs (SEM, secondary electron mode) of the aluminium hydroxide in different conditions: irradiated (in the middle), re-corroded irradiated (on the top right) and unirradiated (on the bottom right)

As illustrated by Fig. 4, after re-corrosion, at 11 days, the hydroxide thickness is larger for irradiated samples than for the unirradiated ones. The increase of the inner layer thickness in particular is very important after ion irradiation and re-corrosion. This inner layer seems to contain the former layers of bayerite and pseudo-boehmite of the hydroxide before the irradiation.

In addition, the ion irradiation seems to increase the kinetics oxidation of aluminium matrix (Fig 4): the ion irradiation degrades the hydroxide film by creating voids, by dehydrating and by amorphizing it. The irradiated film does not protect the matrix. As a result, the oxidation of the aluminium matrix is more important after irradiation compared to the unirradiated samples and it causes the observed increase of hydroxide thickness for 11 days of corrosion in Fig. 4.

#### 4. Discussion

In the literature [1], [19], without irradiation, the mechanism of aluminium corrosion is the following:

1. The aluminium of the matrix is oxidised at the interface oxide-metal, this oxidation is accompanied by the reduction of water and dioxygen, and the production of OH hydroxide groups. A part of this oxidised aluminium reacts with the OH hydroxide groups to form pseudo-boehmite, the inner layer, at the oxide-metal interface. As a result, the inner layer grows by replacing the oxidised aluminium.
2. The rest of the oxidised aluminium is released in solution in the form of ions in the corroding solution. This released material then precipitates at the samples surface to form bayerite, the outer layer.

With the observations made in this study, the following mechanism associated with ion irradiation can be proposed:

1. Before ion irradiation, due to the corrosion test, an hydroxide layer covers the aluminium matrix according to the mechanism described above. These are two pre-existing layers of hydroxide on the surface of the sample.
2. During ion irradiation, the former hydroxide is dehydrated and amorphized. The water of the hydroxide is released because of the vacuum and the ion irradiation. Voids and crystallites of  $\eta$ -Al<sub>2</sub>O<sub>3</sub> can be produced in the hydroxide.
3. After irradiation, during the corrosion test, the irradiated film forms a new inner layer. Due to a bad quality of this irradiated film, the matrix is oxidised and aluminium is released in solution. A new outer layer is formed by the precipitation of aluminium in solution.

However, in this study, we can observe some limitations to the use of ion irradiation to simulate the damage created by the fast neutron flux in reactor.

During the ion irradiation, the hydroxide is irradiated in vacuum. The vacuum and the ion beam led to a dehydration of the hydroxide. The damage due to this dehydration (voids and crystallites of  $\eta$ -Al<sub>2</sub>O<sub>3</sub>) may not be observed in aluminium hydroxide irradiated in a nuclear core.

In addition, to irradiate the hydroxide, the corrosion tests are interrupted, the samples are exposed to air during the break of corrosion tests. Wintergerst observed an effect of breaks during corrosion test: the hydroxide thickness is less important during corrosion tests with breaks than without break [20]. It means the thickness measured in this study may be underestimated because of the break to irradiate the hydroxide.

In addition, we can observe some similarities between ion and neutron irradiation.

On the one hand, AlFeNi samples (composition of the alloy: Fe (0.9 %mass), Ni (0.9 %mass), Cr (0.35 %mass), Mg (1.05 %mass), Al (balance)) were corroded in the BR2 nuclear reactor during 70 days [1]. A XRD analysis performed on the irradiated hydroxide indicates the main crystalline phase is boehmite and traces of bayerite are present. This crystalline composition is the same than that of the re-corroded irradiated hydroxide obtained in this study.

On the other hand, during one year, aluminium samples were corroded in the Osiris nuclear reactor at 45°C and in a corrosion loop at 50°C with similar corrosion conditions. The thickness

of the irradiated hydroxide is about 15 $\mu\text{m}$ , and the thickness of the unirradiated hydroxide is about 3 $\mu\text{m}$ . At low temperature, the neutron irradiation leads to an increase of the hydroxide thickness. In this study, the same observation is made with ion irradiation: irradiation causes an increase of the hydroxide thickness. This increase could be due to the damage in the hydroxide.

To finish, the hydroxide irradiated in nuclear reactor needs more examinations to compared neutron and ion irradiation.

## 5. Conclusion

In this study, Al-Mg-Si alloy samples are corroded at 70°C, in pure water, for 7 days, in order to obtain an aluminium hydroxide film on the samples surface. This hydroxide is composed of two layers: an outer layer in contact with the solution and an inner layer between the outer layer and the aluminium matrix. Micro-crystals of bayerite ( $\alpha\text{-Al(OH)}_3$ ) can be observed in the outer layer. The inner layer is pseudo-boehmite, a nano-crystalline boehmite ( $\gamma\text{-AlOOH}$ ).

The obtained aluminium hydroxide is irradiated with Al ions with successive energies of 1.2 MeV and 5 MeV. The damage created is 2.5 dpa (displacement per atom) on average (SRIM calculation). Ion irradiation induces important changes in the hydroxide: the micro-crystals of bayerite are amorphized. Bubbles and crystallites of  $\eta\text{-Al}_2\text{O}_3$  are produced in the hydroxide.

After ion irradiation, the irradiated oxide is re-corroded in order to evaluate the effect of ion irradiation on the corrosion kinetics. As a result, the hydroxide thickness is larger for the irradiated samples than for the unirradiated ones. The increase of the inner layer thickness in particular is very important after ion irradiation and re-corrosion. Indeed, the ion irradiation degrades the hydroxide film by creating voids, by dehydrating it and by amorphizing it. The irradiated film does not protect the matrix. As a result, the oxidation of the aluminium matrix is more important after irradiation compared to the unirradiated samples.

To finish, during corrosion test in nuclear reactor, a Si-enrichment of the hydroxide is observed [20]. This silicon comes from the aluminium transmuted in silicon because of the thermal neutron flux. In this study, the hydroxide is irradiated with Al ions; it is not enriched with silicon. As a result, a further study will be done with an aluminium hydroxide irradiated with Si ions to simulate the Si-enrichment in order to better understand the role of the silicon in the corrosion process.

## References

- [1] M. Wintergerst, « Etude des mécanismes et des cinétiques de corrosion aqueuse de l'alliage d'aluminium AlFeNi utilisé comme gainage du combustible nucléaire de réacteurs expérimentaux. », Thèse de doctorat, Université Paris XI, U.F.R Scientifique d'orsay, Saclay, 2010.
- [2] C. Vargel, *Corrosion de l'aluminium*. Dunod, 1999.
- [3] S. J. Pawel, D. K. Felde, et R. E. Pawel, « Influence of coolant pH on corrosion of 6061 aluminium under reactor heat transfer conditions », Oak Ridge, TN, USA, 1995.
- [4] S. J. Pawel, G. L. Yoder, D. K. Felde, B. H. Montgomery, et M. T. McFee, « The corrosion of 6061 aluminium under heat transfer conditions in the ANS corrosion test loop », *Oxidation of Metals*, vol. 36, n° 1/2, p. 175-194, 1991.
- [5] S. J. Pawel, G. L. Yoder, C. D. West, et B. H. Montgomery, « The development of a preliminary correlation of data on oxide growth on 6061 aluminium under ANS thermal-hydraulic conditions », *ORNL/TM-11517*, 1990.
- [6] J. C. Griess, H. C. Savage, T. H. Mauney, et J. L. English, « Effect of heat flux on the corrosion of aluminium by water. Part I: Experimental equipment and preliminary results », Oak Ridge, TN, USA, 1960.
- [7] J. C. Griess, H. C. Savage, T. H. Mauney, J. L. English, et J. G. Rainwater, « Effect of heat flux on the corrosion of aluminium by water. Part II: Influence of water temperature, velocity and pH on corrosion-product formation », Oak Ridge, TN, USA, 1961.

- [8] J. C. Griess, H. C. Savage, T. H. Mauney, J. L. English, et J. G. Rainwater, « Effect of heat flux on the corrosion of aluminium by water. Part III : Final report on tests relative of the high-flux isotop reactor », Oak Ridge, TN, USA, 1961.
- [9] J. C. Griess, H. C. Savage, et J. L. English, « Effect of heat flux on the corrosion of aluminium by water. Part IV : Tests relative to the advanced test reactor and correlation with previous results », Oak Ridge, TN, USA, 1964.
- [10] Y. S. Kim, G. L. Hofman, A. B. Robinson, J. L. Snelgrove, et N. Hanan, « Oxidation of aluminum alloy cladding for research and test reactor fuel », *J. Nucl. Mater.*, vol. 378, n° 2, p. 220-228, août 2008.
- [11] Y. Shen, « Comportement et endommagement des alliages d'aluminium 6061-T6 : approche micrométrique », Thèse de doctorat, Ecole Nationale Supérieure des Mines de Paris, 2012.
- [12] S. . Zinkle et G. . Pells, « Microstructure of Al<sub>2</sub>O<sub>3</sub> and MgAl<sub>2</sub>O<sub>4</sub> irradiated at low temperatures », *J. Nucl. Mater.*, vol. 253, n° 1, p. 120-132, mars 1998.
- [13] H. D. Ruan, R. L. Frost, et J. T. Kloprogge, « Comparison of Raman spectra in characterizing gibbsite, bayerite, diaspore and boehmite », *J. Raman Spectrosc.*, vol. 32, n° 9, p. 745-750, sept. 2001.
- [14] C. J. Doss et R. Zallen, « Raman studies of sol-gel alumina: Finite-size effects in nanocrystalline AlO(OH) », *Phys Rev B*, vol. 48, p. 626-637, 1993.
- [15] K. Wefers et C. Misra, *Oxides and hydroxides of aluminium*. ALCOA Laboratories, 1987.
- [16] D. B. Tilley et R. A. Eggleton, « The Natural Occurrence of Eta-Alumina (eta-Al<sub>2</sub>O<sub>3</sub>) in Bauxite », *Clays Clay Miner.*, vol. 44, janv. 1996.
- [17] Y. Chen, J. Hyldtoft, C. J. . Jacobsen, et O. F. Nielsen, « NIR FT Raman spectroscopic studies of η-Al<sub>2</sub>O<sub>3</sub> and Mo/η-Al<sub>2</sub>O<sub>3</sub> catalysts », *Spectrochim. Acta. A. Mol. Biomol. Spectrosc.*, vol. 51, n° 12, p. 2161-2169, nov. 1995.
- [18] R. W. G. Wyckoff, *Crystal structures*, Arizona. Wiley (Interscience)., vol. 1. Second edition. University of Arizona, Tucson, 1965.
- [19] R. K. Hart, « The formation of films on aluminium immersed in water », *Trans Faraday Soc*, vol. 53, p. 1020-1025, 1956.
- [20] M. Wintergerst, N. Dacheux, F. Datcharry, E. Herms, et B. Kapusta, « Corrosion of the AlFeNi alloy used for the fuel cladding in the Jules Horowitz research reactor », *J. Nucl. Mater.*, vol. 393, n° 3, p. 369-380, sept. 2009.